Because this uncovered region is uncovered only when a fibrin clot forms and the amino acid sequence of the epitope of the 102–10 mAb is completely conserved in mammals, the 102–10 mAb and other mAbs developed against human fibrin clots cross-reacted with mouse or rat fibrin clots. Therefore, we investigated the fate of fibrin clots in mice or rats using disease models, such as models of cerebral infarction, incisional wounds, and arthritis (Fig. 3a). These results indicated that fibrin clot formation occurred only in the acute phase of non-malignant diseases, including thrombosis, inflammation, and trauma, and these clots virtually disappeared within 2 to 3 weeks and were substituted by collagen in the late phase. We next synthesised a positron emission tomography (PET) probe of ^{89}Zr-labelled 102–10 (Fig. 3b), which was injected into mice bearing chemically induced spontaneous cutaneous tumours generated using 7,12-dimethylbenz[a]anthracene (DMBA) as an initiator and phorbol 12-myristate 13-acetate (PMA) as a promoter[25]. This spontaneous tumour was selected as an appropriate experimental model to evaluate our immuno-probe because it exhibits remarkable fibrin deposition and abundant interstitial tissue, similar to clinical human cancers and unlike human tumour xenografts in mice[26]. The 102–10 mAb probe showed clear and more specific accumulation in tumours compared to cetuximab (control), as assessed by computerized tomography (CT) scan (Fig. 3c, Supplementary Fig. 3). Next, we histologically evaluated the specificity of the 102–10 mAb probe within the tumour tissue. Haematoxylin and eosin (HE) staining showed that the tumour consisted of areas with basophilic tumour cells and eosinophilic tumour stroma, and the accumulation of the 102–10 mAb probe was more pronounced in fibrin clot-positive

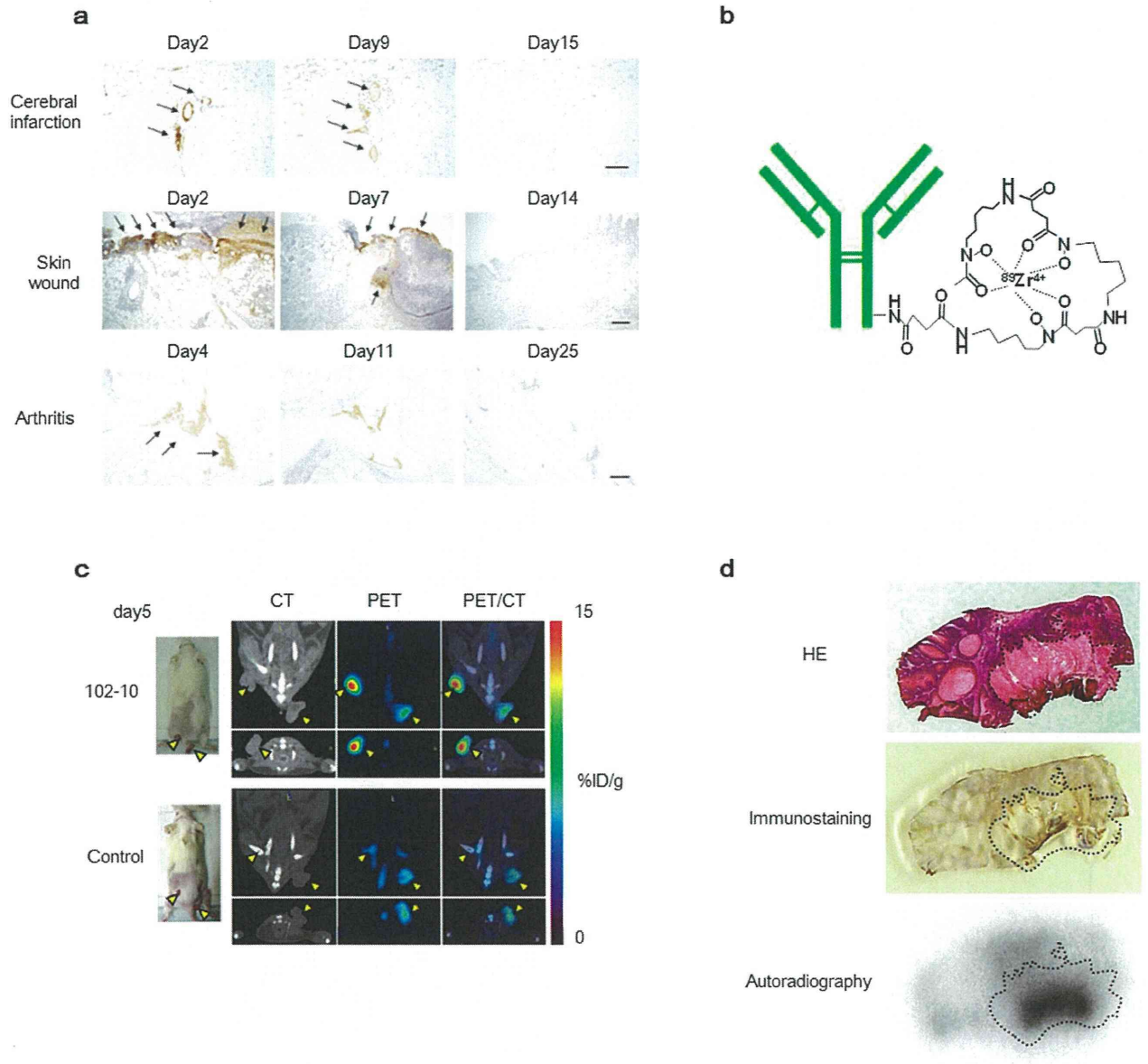

Figure 3 | The kinetics of fibrin clot deposition in several non-malignant disease models and PET/CT with ^{89}Zr-labelled 102–10 in spontaneous tumour models. (a) The kinetics of fibrin clot deposition in rat cerebral infarction (upper), mouse incisional wound (middle), and mouse arthritis (lower) were evaluated immunohistochemically. Fibrin clot deposition was observed at the acute phase (left and middle) but not at the late phase (right). Scale bar, 100 μm. (b) The PET probe was composed of the 102–10 mAb, a linker, and ^{89}Zr. (c) The ^{89}Zr-labelled 102–10 mAb probe showed clearer and more specific accumulation in tumours as compared to the control (cetuximab). The yellow arrows indicated tumours. (d) The 102–10 mAb probe accumulated within fibrin-positive tumour stroma, as represented by the dashed line.

tumour stroma (Fig. 3d). These PET/CT data from mouse experiments can be reasonably extrapolated to humans because the 102–10 mAb can recognise both human and mouse fibrin clots, and humans and mice show common features of fibrin deposition.

To evaluate the reactivity of the 102–10 mAb to intravital fibrin clots under various conditions in humans, normal tissue and tissues from non-malignant and malignant diseases were stained with the 102–10 mAb. Strong fibrin deposition was observed in almost all cancer tissues, including brain, lung, pancreatic, and colorectal cancers, but not in normal tissues (Fig. 4a and Supplementary Table 1). In cases of non-malignant disease, fibrin clots were detected at the onset of cerebral infarction and cardiac infarction or in cases of serious inflammation, such as acute pancreatitis (Supplementary Table 1). However, no clear fibrin clots were detected in the late or chronic phases of non-malignant conditions following the digestion of fibrin clots by plasmin and replacement by collagenous tissue (Fig. 4b).

Erosive types of cancer are known to be more destructive, resulting in higher fibrin clot deposition. In this context, we closely investigated fibrin deposition in surgically resected samples of glioma, one of the most erosive tumour types. Immunohistochemistry was conducted for WHO-classified glioma tissue samples, and the level of fibrin deposition was graded into three subgroups: (−) fibrin clot not detectable, (+) faint but clear deposition, or (++) strong heterogeneous or diffuse deposition (Fig. 4c). Fibrin deposition was observed in 100% (20/20) of grade 4 gliomas (glioblastoma multiforme (GBM)), with strong fibrin deposition observed in 65% of cases (13/20). In grade 3 gliomas, fibrin deposition was observed in 40% of cases (8/20), with strong fibrin deposition observed in 10% of cases (2/20). In grade 1/2 gliomas, fibrin deposition was observed in 60% of cases (12/20), and strong fibrin deposition was observed in 10% of cases (2/20) (Fig. 4d).

Discussion

Combining previous lines of clinicopathological evidence with our present data, even tiny and asymptomatic tumours will likely become aggressively malignant if they are detected by PET/CT using the radiolabelled 102–10 mAb. The deposition of fibrin in non-malignant disease is inevitably accompanied by various symptoms related to the particular pathology, such as infarction or inflammation. Conversely, tumour-related fibrin deposition is not associated with any symptoms, even in patients with stage 4 disease. When a cancer diagnosis is accompanied by symptoms, such as pain or macroscopic bleeding, the cancer likely involves sensory nerves and the destruction of bone and large blood vessels, which is generally observed in patients with end-stage cancer. Therefore, earlier detection of cancers at the asymptomatic stage using mAbs is important to achieve a favourable clinical outcome[27].

The biological significance of tumour fibrin clots has been gradually elucidated, as several growth factors that preserve the fibrin matrix have been shown to promote tumour cell growth, angiogenesis[28], and metastasis[27,29]. Conversely, the role of fibrin clots in the tumour stroma has yet to be definitively characterised. Here, we discovered an uncovered region that develops in the fibrin clot during its formation, and we generated mAbs that bound exclusively to fibrin clots. The specificity of the 102–10 mAb to fibrin clots was verified by the present ELISA and western blot (Figure 1a,

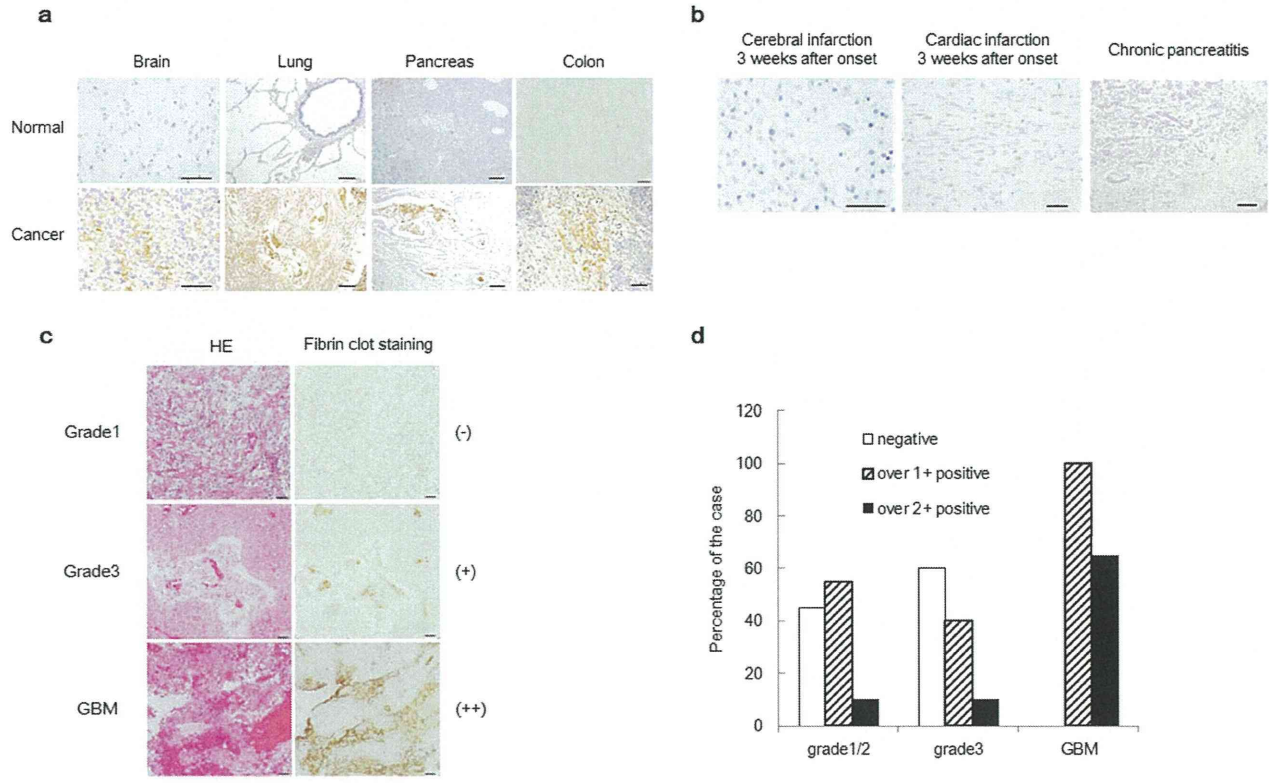

Figure 4 | Immunostaining of fibrin clots in various human tissues and the fibrin clot status according to WHO-classified glioma grade. (a, b) Fibrin deposition was strongly detected in human cancer tissues but not in normal human tissues or during the late or chronic phases of non-malignant diseases. Scale bar, 100 μm. (c) Immunohistochemical analysis of glioma. The left panels show HE staining, and the right panels show fibrin clot staining. The level of fibrin deposition was graded into 3 subgroups: (−) undetectable fibrin clot (upper panel, grade1); (+) faint but clear deposition (middle panel, grade3); or (++) strong heterogeneous or diffuse deposition (lower panel, GBM). (d) The percentage of fibrin deposition is shown. The clinical stages of the patients were classified as grade 1/2, grade 3, or grade 4 (GBM) according to the WHO grade classification. Each group consisted of 20 cases.

supplementary Fig. 1c, and 4). Therefore, the 102–10 mAb may not be neutralised by fibrinogen, soluble fibrin, or D-dimer in the bloodstream due to its unique properties.

Our immunohistochemical and PET/CT findings using these newly developed anti-insoluble-fibrin mAbs, including 102–10, further demonstrated that these mAbs could be used to detect high-grade, aggressive, malignant tumours. Further development of such a method to detect fibrin clots is therefore desirable from an oncological perspective.

Methods

Production of the 102–10 mAb. We developed our anti-human fibrin mAb by converting fibrinogen (Sigma, St Louis, MO) into a fibrin clot via thrombin (Sigma) cleavage. The fibrin was frozen in liquid nitrogen and crushed, and the crushed fibrin was then suspended in saline and used to immunise mice. Lymph node cells from an immunised mouse were fused with myeloma cells (P3U1), and specific antibody-producing hybridoma clones were selected by ELISA as described previously[13].

Enzyme-linked immunosorbent assay (ELISA). The reference standards for soluble fibrin and D-dimer were obtained from Sekisui Medical (Tokyo, Japan). One microgram of antigen was immobilised onto a 96-well plate for 12 hours. The fibrinogen-immobilised plates were then treated with a thrombin solution at 37°C for 1 hour to prepare the fibrin clot plates, as described previously[20]. The wells were then blocked using N102 (Nichiyu, Tokyo, Japan) for 3 hours. Subsequently, the plates were incubated in 1 μg/mL peroxidase-conjugated mAb 1 hour, and the wells were washed with Tris-buffered saline (TBS) containing 0.05% Tween 20 (TBS-T). Finally, the mAbs bound to the wells were visualised using a 1-Step Slow TMB-ELISA (Thermo, Waltham, MA, USA) as a substrate for 30 minutes.

Western blot. The mAbs were first conjugated to peroxidase (Dojindo, Kumamoto, Japan). One microgram of fibrinogen or its proteolytic product sample was obtained by Sodium dodecyl sulphate polyaclylamide gel electrophoresis (SDS-PAGE) under reducing, heat-shocked, or untreated conditions. The proteins were then electrophoretically transferred to polyvinylidenedifluoride (PVDF) membranes (Bio-Rad, Hercules, CA, USA) using the Trans-Blot Turbo transfer machine (Bio-Rad). The membranes were then placed in a protein detection system (SNAP i.d.; Millipore, Billerica, MA, USA) and blocked with phosphate-buffered saline (PBS) containing 0.3% Difco skim milk (Becton Dickinson, Franklin Lakes, NJ, USA) and 0.1% Tween 20 (PBS-T, Sigma). The membranes were then incubated in 2 μg/mL peroxidase-conjugated mAbs with 0.3% skim milk in 0.1% PBS-T for 10 min at room temperature. Subsequently, the membranes were washed with TBS-T. Finally, the proteins on the membrane were visualised using ECL prime (GE Healthcare, Piscataway, NJ, USA) as a substrate. After analysis in a ChemiDoc imager (Bio-Rad), the membrane was stained with Quick CBB (Wako Pure Chemical Industries, Osaka, Japan).

Isolation of fibrinogen Bβ chain. Five micrograms of fibrinogen were separated by SDS-PAGE under reducing conditions. The polyacrylamide gel was then stained with EZ Stain reverse (ATTO, Tokyo, Japan). The fibrinogen Bβ chain fraction was cut out from the polyacrylamide gel, followed by extraction of the protein using an Atto prep MF column (ATTO).

Limited digestion with lysyl endopeptidase and protein sequencing. Lysyl endopeptidase (Wako Pure Chemical Industries) digestion of the fibrinogen Bβ chain protein was carried out in PBS (pH 7.4) with a protein:enzyme ratio (w/w) of 45 : 1 at 37°C for 6 hours, and the digested peptide was separated by SDS-PAGE electrophoresis under reducing conditions. The fragments were detected by western blot, and the minimum positive band (approximately 10 kDa) was obtained using the method described above. The amino acid sequence of the 10-kDa peptide was determined using a PPSQ-33A protein sequencer (Shimadzu, Kyoto, Japan).

Inhibition of 102–10 binding to fibrin clots using a series of synthetic peptides. Five synthetic peptides [No. 1 (Bβ149–178), No. 2 (Bβ179–208), No. 3 (Bβ209–234), No. 4 (Bβ170–186), and No. 5 (Bβ201–216)] were prepared using the amino acid sequence of the 10-kDa peptide (Sigma). A PBS solution containing 1 μg/mL peroxidase-conjugated 102–10 was then mixed with diluted synthetic peptides (0.01–100 μM), and the mixture was incubated for 1 hour at 37°C. After discarding the blocking reagent, 100 μL of the mixture was applied to a fibrin-coated 96-well plate[17]. Subsequently, the wells were washed with TBS-T, and the antibodies in the wells were visualised using the 1-Step Slow TMB ELISA as a substrate for 5 minutes.

Producing the anti-Bβ chain and anti-γ chain mAbs. The crystal structure of fibrinogen (3GHG) was obtained from the RCSB Protein Data Bank (http://www.rcsb.org/pdb/home/home.do) and visualised using PyMOL ver1.3r1 edu (http://www.pymol.org/pymol). To produce new antibodies that recognise epitope regions of the fibrin clot Bβ chain (CNIPVVSGKECEEIIR) or γ chain (KNWIQYKEGFGHLSP), recombinant epitope protein was produced from pET21b (Novagen, Darmstadt, Germany) and fibrinogen Bβ chain DNA or fibrinogen γ chain DNA (Origene Technology, Rockville, MD). Six-week-old BALB/cAnNCrlCrlj mice (Charles River Japan, Yokohama, Japan) were immunised intraperitoneally (i.p.) with an emulsion of Freund's complete adjuvant (DIFCO, Franklin Lakes, NJ, USA) and a saline solution containing 50 μg of the Bβ chain of the epitope peptide with a 4M-tag (Bio Matrix Research, Inc., Chiba, Japan). Three to five successive booster injections were administered i.p. at 2-week intervals using the same amount of antigen in an adjuvant system (Sigma). A final boost was provided by administering the same amount of antigen intravenously. An antibody recognising the γ chain of the fibrin clot was produced by ITM Co. Ltd (Matsumoto, Japan). The specificity of the obtained mAbs against the epitope regions of the Bβ and γ chains was evaluated by ELISA.

Hydrophobic, ionic, and hydrogen bonds between the Bβ chain and γ chain in the unique region of fibrin clots. Electrostatic surface representations (−5 kT/e, red, to +5 kT/e, blue) of the Bβ chain and γ chain were generated using the APBS software package (https://sites.google.com/a/poissonboltzmann.org/software/apbs), and the images of all molecular structures were displayed in PyMOL ver1.3r1 edu.

Immunohistochemistry. Non-malignant human tissues were obtained from Fukushima Medical University. Glioma samples were obtained from Kumamoto University. Immunohistochemical studies in human tissue samples were conducted on surgically resected tissue samples and tissue samples obtained from autopsy. All samples were collected according to an institutional review board-approved protocol. Tissue sections from paraffin-embedded tissue samples were prepared, and heat-induced antigen retrieval was performed at 120°C for 10 minutes in 10 mM citrate (pH 6). After blocking with 5% skim milk in PBS, the sections were incubated with the 102–10 mAb for 1 to 2 hours at room temperature or overnight at 4°C. After washing with PBS, the sections were then incubated with peroxidase-conjugated anti-human IgG secondary antibody (MBL Co., Ltd., Nagoya, Japan) for 60 minutes. The reaction was visualised using DAB (Dako, Glostrup, Denmark), and the slides were counterstained with haematoxylin.

PET/CT imaging and autoradiography using ^{89}Zr-labelled 102–10. The 102–10 mAb was conjugated to *p*-isothiocyanatobenzyl-desferrioxamine B (DF) as previously described[30]. The conjugation ratio of DF to IgG was estimated to be 1.0 to 1.3, as determined by size-exclusion chromatography using a PD10 column (GE Healthcare). The nonconjugated chelate was removed using a Sephadex G-50 spin column (GE Healthcare). ^{89}Zr-oxalate was produced using a cyclotron at the National Institute of Radiological Sciences (Chiba, Japan) as previously described[31]. The DF-conjugated 102–10 mAb (100 μg in 20 μL of PBS) was incubated with 5.0 to 5.6 MBq of ^{89}Zr-oxalate (3.7–5.6 GBq/mL, pH 7–9) for 1 hour at room temperature. The radiolabelled 102–10 mAb was purified using a Sephadex G-50 spin column. The radiochemical yield of ^{89}Zr-labelled IgG was between 73 and 96%, the radiochemical purity was between 96 and 98%, and the specific activity was between 37 and 44 kBq/μg as determined by thin-layer chromatography using 50 mM diethylene triamine pentaacetic acid (DTPA, pH 7) as the mobile phase.

Mice were injected with approximately 3.7 MBq of ^{89}Zr-labelled 102–10 mAb into the tail vein. The injected protein dose was adjusted to 100 μg per mouse by the addition of unlabelled antibody. The PET data were acquired for 10 to 20 minutes using a small-animal PET system (Inveon, Munich, Germany) under isoflurane anaesthesia. Body temperature was maintained at 37°C using a lamp and a heating pad during the scan. The images were reconstructed using 3D maximum a posteriori (18 iterations with 16 subsets, β = 0.2 resolution) without attenuation correction. The tracer uptake was expressed as the percentage of the injected dose per gram of tissue (% ID/g). After PET scanning, the CT images were acquired with an X-ray source set at 90 kVp and 200 μA using a small-animal CT system (R_mCT2, Rigaku, Tokyo, Japan). After imaging, the mice were euthanised, and the tumours were excised and quickly frozen in an optimal-cutting-temperature (OCT) compound (Sakura Finetek Japan, Tokyo, Japan). The dried sections (20 μm thick) were exposed to an imaging plate (Fuji Film, Tokyo, Japan) and then stained with HE.

Animal model. Chemical skin carcinogenesis was induced as previously described[26,32–34]. Briefly, 7,12-dimethylbenz[a]anthracene (DMBA; 250 μg/mL in acetone; Sigma) was applied once to the shaved dorsal skin of the mice as an initiator. After 1 week, phorbol 12-myristate 13-acetate (PMA; 25 μg/mL in acetone; Sigma) was applied weekly (for a total of 32 times) as a promoter. All animal procedures and experiments were approved by the Committee for Animal Experimentation of the National Cancer Centre, Tokyo Japan.

Statistical analysis. A two-sided Student's *t*-test was used to compare the two groups. Steel's test was used to compare multiple groups with Statcel3 (OMS, Saitama, Japan). A two-factor factorial analysis of variance was used to evaluate the inhibition effect.

1. Mosesson, M. W. Fibrinogen and fibrin structure and functions. *J Thromb Haemost* **3**, 1894–1904 (2005).
2. Pacella, B. L., Jr., Hui, K. Y., Haber, E. & Matsueda, G. R. Induction of fibrin-specific antibodies by immunization with synthetic peptides that correspond to amino termini of thrombin cleavage sites. *Mol Immunol* **20**, 521–527 (1983).
3. Brass, E. P., Forman, W. B., Edwards, R. V. & Lindan, O. Fibrin formation: the role of the fibrinogen-fibrin monomer complex. *Thromb Haemost* **36**, 37–48 (1976).
4. Graeff, H., Hafter, R. & von Hugo, R. On soluble fibrinogen-fibrin complexes. *Thromb Res* **16**, 575–576 (1979).

5. Drew, A. F., Liu, H., Davidson, J. M., Daugherty, C. C. & Degen, J. L. Wound-healing defects in mice lacking fibrinogen. *Blood* **97**, 3691–3698 (2001).
6. Silvain, J. *et al.* Composition of coronary thrombus in acute myocardial infarction. *Journal of the American College of Cardiology* **57**, 1359–1367 (2011).
7. Skaf, E. *et al.* Venous thromboembolism in patients with ischemic and hemorrhagic stroke. *Am J Cardiol* **96**, 1731–1733 (2005).
8. Levi, M., van der Poll, T. & Buller, H. R. Bidirectional relation between inflammation and coagulation. *Circulation* **109**, 2698–2704 (2004).
9. Idell, S. *et al.* Regulation of fibrin deposition by malignant mesothelioma. *Am J Pathol* **147**, 1318–1329 (1995).
10. Im, J. H. *et al.* Coagulation facilitates tumour cell spreading in the pulmonary vasculature during early metastatic colony formation. *Cancer Res* **64**, 8613–8619 (2004).
11. Dvorak, H. F. Tumors: wounds that do not heal. Similarities between tumour stroma generation and wound healing. *N Engl J Med* **315**, 1650–1659 (1986).
12. Matsumura, Y. Cancer stromal targeting (CAST) therapy. *Adv Drug Deliv Rev* **64**, 710–719 (2012).
13. Yasunaga, M., Manabe, S. & Matsumura, Y. New concept of cytotoxic immunoconjugate therapy targeting cancer-induced fibrin clots. *Cancer Sci* **102**, 1396–1402 (2011).
14. Soe, G., Kohno, I., Inuzuka, K., Itoh, Y. & Matsuda, M. A monoclonal antibody that recognizes a neo-antigen exposed in the E domain of fibrin monomer complexed with fibrinogen or its derivatives: its application to the measurement of soluble fibrin in plasma. *Blood* **88**, 2109–2117 (1996).
15. Wada, H. *et al.* Elevated levels of soluble fibrin or D-dimer indicate high risk of thrombosis. *J Thromb Haemost* **4**, 1253–1258 (2006).
16. Laudano, A. P. & Doolittle, R. F. Synthetic peptide derivatives that bind to fibrinogen and prevent the polymerization of fibrin monomers. *Proc Natl Acad Sci U S A* **75**, 3085–3089 (1978).
17. Kudryk, B., Rohoza, A., Ahadi, M., Chin, J. & Wiebe, M. E. A monoclonal antibody with ability to distinguish between NH2-terminal fragments derived from fibrinogen and fibrin. *Mol Immunol* **20**, 1191–1200 (1983).
18. Scheefers-Borchel, U., Muller-Berghaus, G., Fuhge, P., Eberle, R. & Heimburger, N. Discrimination between fibrin and fibrinogen by a monoclonal antibody against a synthetic peptide. *Proc Natl Acad Sci U S A* **82**, 7091–7095 (1985).
19. Schielen, W. J., Voskuilen, M., Tesser, G. I. & Nieuwenhuizen, W. The sequence A alpha-(148-160) in fibrin, but not in fibrinogen, is accessible to monoclonal antibodies. *Proc Natl Acad Sci U S A* **86**, 8951–8954 (1989).
20. Gargan, P. E., Graffney, P. J., Pleasants, J. R. & Ploplis, V. A. A Monoclonal Antibody which Recognises an Epitopic Region Unique to the Intact Fibrin Polymeric Structure. *Fibrinolysis* **7**, 275–283 (1993).
21. Hui, K. Y., Haber, E. & Matsueda, G. R. Monoclonal antibodies to a synthetic fibrin-like peptide bind to human fibrin but not fibrinogen. *Science* **222**, 1129–1132 (1983).
22. Kudryk, B., Rohoza, A., Ahadi, M., Chin, J. & Wiebe, M. E. Specificity of a monoclonal antibody for the NH2-terminal region of fibrin. *Mol Immunol* **21**, 89–94 (1984).
23. Rosebrough, S. F. *et al.* Aged venous thrombi: radioimmunoimaging with fibrin-specific monoclonal antibody. *Radiology* **162**, 575–577 (1987).
24. Kollman, J. M., Pandi, L., Sawaya, M. R., Riley, M. & Doolittle, R. F. Crystal structure of human fibrinogen. *Biochemistry* **48**, 3877–3886 (2009).
25. Filler, R. B., Roberts, S. J. & Girardi, M. Cutaneous two-stage chemical carcinogenesis. *CSH Protoc* **2007**, pdb prot4837 (2007).
26. Hirakawa, S. *et al.* VEGF-A induces tumour and sentinel lymph node lymphangiogenesis and promotes lymphatic metastasis. *The Journal of experimental medicine* **201**, 1089–1099 (2005).
27. Prandoni, P., Falanga, A. & Piccioli, A. Cancer and venous thromboembolism. *Lancet Oncol* **6**, 401–410 (2005).
28. Fernandez, P. M., Patierno, S. R. & Rickles, F. R. Tissue factor and fibrin in tumour angiogenesis. *Semin Thromb Hemost* **30**, 31–44 (2004).
29. Palumbo, J. S. *et al.* Fibrinogen is an important determinant of the metastatic potential of circulating tumour cells. *Blood* **96**, 3302–3309 (2000).
30. Perk, L. R. *et al.* p-Isothiocyanatobenzyl-desferrioxamine: a new bifunctional chelate for facile radiolabeling of monoclonal antibodies with zirconium-89 for immuno-PET imaging. *Eur J Nucl Med Mol Imaging* **37**, 250–259 (2010).
31. Nagatsu, K. *et al.* An alumina ceramic target vessel for the remote production of metallic radionuclides by in situ target dissolution. *Nuclear medicine and biology* **39**, 1281–1285 (2012).
32. Takano, K., Tatlisumak, T., Bergmann, A. G., Gibson, D. G., 3rd. & Fisher, M. Reproducibility and reliability of middle cerebral artery occlusion using a silicone-coated suture (Koizumi) in rats. *J Neurol Sci* **153**, 8–11 (1997).
33. Hutamekalin, P. *et al.* Collagen antibody-induced arthritis in mice: development of a new arthritogenic 5-clone cocktail of monoclonal anti-type II collagen antibodies. *J Immunol Methods* **343**, 49–55 (2009).
34. Basu, A., Kligman, L. H., Samulewicz, S. J. & Howe, C. C. Impaired wound healing in mice deficient in a matricellular protein SPARC (osteonectin, BM-40). *BMC Cell Biol* **2**, 15 (2001).

Acknowledgments

This work was supported by the National Cancer Centre Research and Development Fund (Y.M.); the Funding Program for World-Leading Innovative R&D in Science and Technology (FIRST Program) (Y.M.); the Third Term Comprehensive Control Research for Cancer from the Ministry of Health, Labour, and Welfare of Japan (Y.M.); a Grant-in-Aid for Scientific Research or Priority Areas from the Ministry of Education, Culture, Sports, Science, and Technology; the Princess Takamatsu Cancer Research Fund (Y.M.); and the Japanese Foundation for Multidisciplinary Treatment of Cancer (Y.M.). We thank Dr. S. Iwanaga for his expertise. We also thank Ms. M. Takigahira for her assistance with the animal experiments, Mrs. H. Koike and Mrs. M. Araake-Mizoguchi for their assistance with producing the 102–10 mAb, and Mrs. K. Shiina for secretarial support.

Author contributions

Y.M. provided the original concept for the research and the anti-fibrin clot monoclonal antibody (102–10). Y.H., M.Y. and Y.M. designed the study. Y.H., M.Y., S.H., S.S., T.S., T.S. and A.T. performed the experiments. Y.H., M.Y., S.H., S.S., T.S., A.T., T.S., K.T., S.M., J.K., J.K. and Y.M. discussed the results and wrote the paper.

Additional information

Supplementary information accompanies this paper at http://www.nature.com/scientificreports

Competing financial interests: The authors declare no competing financial interests.

How to cite this article: Hisada, Y. *et al.* Discovery of an uncovered region in fibrin clots and its clinical significance. *Sci. Rep.* 3, 2604; DOI:10.1038/srep02604 (2013).

Chapter 6
Cancer Stromal Targeting (CAST) Therapy and Tailored Antibody Drug Conjugate Therapy Depending on the Nature of Tumor Stroma

Yasuhiro Matsumura, Masahiro Yasunaga, and Shino Manabe

Abstract In spite of recent success of monoclonal antibody (mAb) drug conjugate (ADC) therapy in patients with hypervascular and special tumors recognized by a particular mAb, there are several issues to be solved for ADC counted as universal therapy for any types of cancer. Especially most human solid tumors possess abundant stroma that hinders the distribution of ADC. To overcome these drawbacks, we developed a unique strategy that the cancer stromal targeting (CAST) therapy by cytotoxic immunoconjugate bound to the collagen IV or fibrin network in the tumor stroma from which the payload is released gradually and distributed throughout the tumor, resulting in the arrest of tumor growth due to induced damage to tumor cells and tumor vessels.

In addition to the CAST therapy, we clarified the appropriate combination of targeting antibody and conjugate design of antitumor immunoconjugate depending on a quantity of tumor stroma. Hence, we selected two types of conjugate linker, ester bond and carbamate bond. It was found that combination of stromal targeting mAb and a linker composed of ester bond to release drug outside the cells was effective against the stroma-rich cancer. Conversely, cancer cell targeting via carbamate bond to release drug inside the cells was effective against stroma-poor cancer. It seemed that outcome of ADC therapy against each individual tumor having distinct stromal structure was dependent on the selection of conjugation design, as well as targeting mAb.

Y. Matsumura, M.D., Ph.D. (✉) • M. Yasunaga
Division of Developmental Therapeutics, National Cancer Center Hospital East, Kashiwa, Chiba, Japan
e-mail: yhmatsum@east.ncc.go.jp

S. Manabe
Synthetic Cellular Chemistry Laboratory, RIKEN, Wako, Saitama, Japan

Y.H. Bae et al. (eds.), *Cancer Targeted Drug Delivery: An Elusive Dream*,
DOI 10.1007/978-1-4614-7876-8_6,

Introduction

There are two main concepts in DDS, active targeting and passive targeting. Active targeting involves monoclonal antibodies (mAb) or ligands to tumor-related receptors which can target the tumor by utilizing the specific binding ability between the antibody and antigen or between the ligand and its receptor. The passive targeting system can be achieved by the EPR effect, that is, the enhanced permeability and retention effect [1–3]. Small molecules easily leak from normal vessels in the body, which gives small molecules a short plasma half-life. On the other hand, macromolecules have a long plasma half-life because they are too large to pass through the normal vessel walls, unless they are trapped by the reticuloendothelial system (RES) in various organs. Solid tumors generally possess several pathophysiological characteristics: hypervasculature, secretion of vascular permeability factors stimulating extravasation of macromolecules within a tumor, and absence of effective lymphatic drainage from tumors that impedes the efficient clearance of macromolecules accumulated in solid tumor tissues.

Macromolecules and lipids in the interstitial tissue are known to be recovered via the lymphatics in normal tissues [4]. The limited recovery from the lymphatic system in tumor tissues may be attributed to poor development of the lymphatics in tumor tissues, which has been demonstrated by using lipid lymphographic agents [5].

Although there is no clear anatomical proof that tumor lymphogenesis is implicated in the drainage of extravasated macromolecules in human, some studies have indicated that the growth of lymphatic vessels is actively involved in tumor dissemination [6].

This inconsistency regarding tumor lymphogenesis may be due to differences between mice and humans, or differences among tumor types. These characteristics of solid tumors are the EPR effect. Based on the EPR effect, several formulations categorized in passive targeting have been developed and some of them such as Doxil [7] and Abraxane [8] have been approved in clinical use, and anticancer agents (ACAs) incorporating micelles and polymer-conjugated ACAs are now under preclinical and clinical evaluation [9–11].

Monoclonal antibody, which can target the tumor cell actively by the specific binding ability against corresponding antigen, easily extravasates from leaky tumor vessels but not from normal vessels, is long retained in the tumor by utilizing active targeting and passive targeting based on the EPR effect. Therefore, numerous mAbs have been developed and conjugated with ACAs or toxins to create "ADC, immunoconjugate strategy" [12–15]. Recent examples of the conjugates include anti-CD33-calicheamicin and anti-CD20-radiolabeled immunoconjugate and were effective to hematological malignancy such as malignant lymphoma and leukemia [12]. Very recently, the phase 3 trial showed that T-DM1 appeared to have a significant survival benefit in HER2-positive breast cancer that is a representative of hypervascular cancers [16]. Heterogeneity of the cancer cells, however, prevents development of the ADC based on cell-specific antigen [17–20]. Moreover, conventional ADCs depend on cleavage of conjugation site with intracellular biochemical (enzymatic) process after the cell uptake of the conjugate [21–24]. In addition to

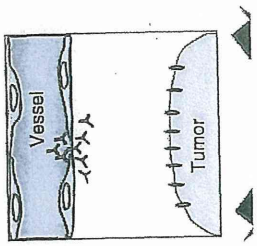

Fig. 6.1 The schema of ar
barrier like malignant lym
internalized after antigen-b
cer (PC) possess stromal b
cells such that antigen-bind

such annoying characte
such as pancreatic can
the distribution of mA
developed a unique str
cytotoxic immunoconju
stroma from which the
tumor, resulting in the
and tumor vessels [29,
immunoconjugate ther
tumor stroma were not

In this context, it is
antibody and conjugate
tity of tumor stroma. F
and carbamate bond. V
mAb and a linker comp
effective against the st
carbamate bond to rele
poor cancer. It seemed
vidual tumor having d
conjugation design, as

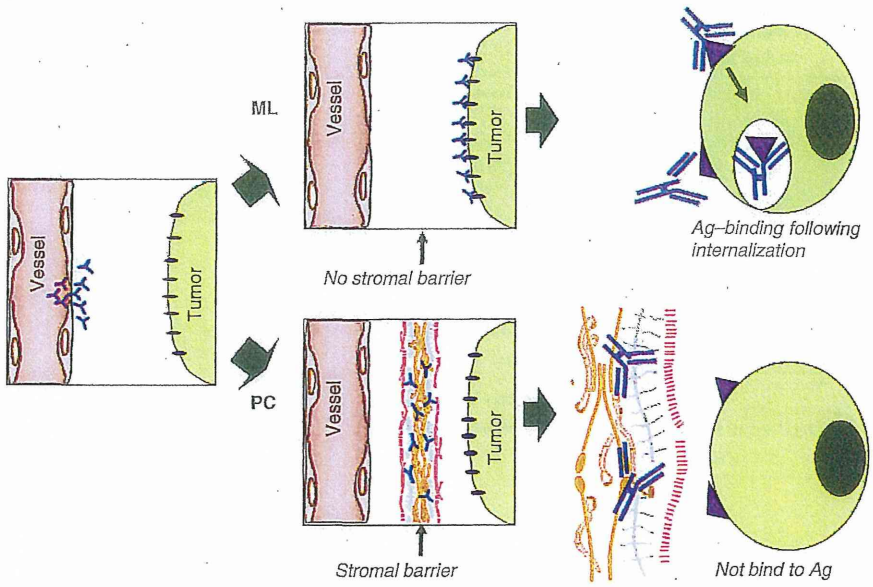

Fig. 6.1 The schema of antibody delivery into the tumor cells. In the tumor having no stromal barrier like malignant lymphoma (ML), antibodies were delivered into the cancer cells, can be internalized after antigen-binding. However, many human solid tumors including pancreatic cancer (PC) possess stromal barrier hindering the distribution of the immunoconjugates into cancer cells such that antigen-binding following antibody-intrernalization never occur. Ag, Antigen

such annoying characteristics of cancer cells themselves, most human solid tumors such as pancreatic cancer and gastric cancer possess abundant stroma that hinders the distribution of mAbs (Fig. 6.1) [25–28]. To overcome these drawbacks, we developed a unique strategy that the cancer stromal targeting (CAST) therapy by cytotoxic immunoconjugate bound to the collagen IV or fibrin network in the tumor stroma from which the payload is released gradually and distributed throughout the tumor, resulting in the arrest of tumor growth due to induced damage to tumor cells and tumor vessels [29, 30]. However, the merit and demerit of anti-stromal targeting immunoconjugate therapy in relation to the conjugate design and the amount of tumor stroma were not yet fully elucidated.

In this context, it is important to clarify the appropriate combination of targeting antibody and conjugate design of antitumor immunoconjugate depending on a quantity of tumor stroma. Hence, we selected two types of conjugate linker, ester bond and carbamate bond. We hypothesized that combination of anti-stromal targeting mAb and a linker composed of ester bond to release ACA outside the cells would be effective against the stroma-rich cancer. Conversely, anticancer cell targeting via carbamate bond to release ACA inside the cells would be effective against stroma-poor cancer. It seemed that outcome of immunoconjugate therapy against each individual tumor having distinct stromal structure was dependent on the selection of conjugation design, as well as targeting mAb.

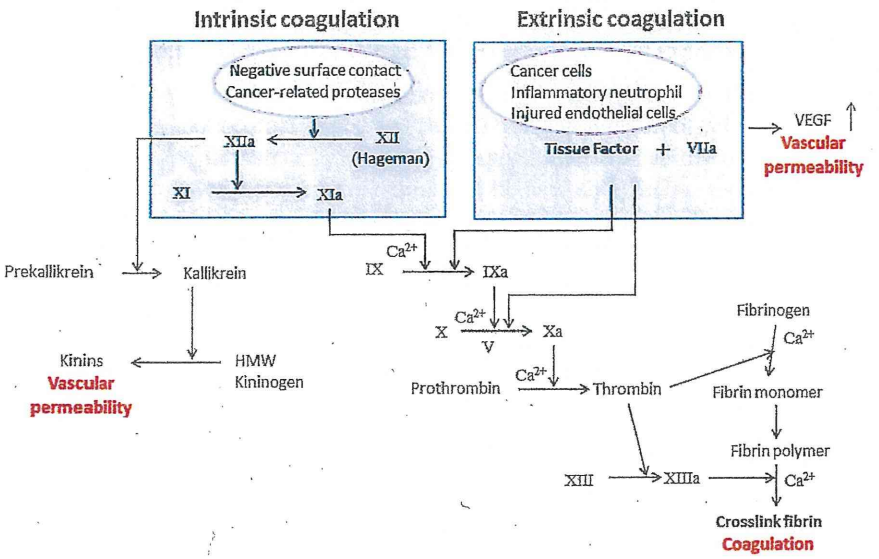

Fig. 6.2 Tumor-induced blood coagulation cascade. Both intrinsic and extrinsic coagulation factors may be involved in tumor vascular permeability

Cancer Stroma

The increased tumor vascular permeability is the most important event for the EPR effect. At the time we proposed the EPR effect, we also succeeded in purifying two types of kinin (bradykinin and hydroxyprolyl^3-bradykinin) from the ascitic fluid of a patient with gastric cancer [1, 31]. We also clarified that this kinin generation system was triggered by the activated Hageman factor, an intrinsic coagulation factor XII [32].

Meanwhile, Dvorak et al. discovered that vascular permeability factor (VPF) was involved in tumor vascular permeability [33]. Later, it was found that VPF was identical to vascular endothelial growth factor (VEGF) [34]. Recently, an extrinsic coagulation factor, namely a tissue factor (TF), appeared to activate VEGF production [35]. So, both intrinsic and extrinsic coagulation factors may be involved in tumor vascular permeability as well as tumor-induced blood coagulation (Fig. 6.2).

In the nineteenth century, French surgeon Armand Trousseau described thrombophlebitis in patients with stomach cancer for the first time [36]. Today, a large body of clinical evidence supports the conclusion that abnormal coagulation occurs in a variety of cancer patients [37]. It is now known that TF is highly expressed on the surface of almost all human cancer cells, and alternatively spliced soluble TF is also produced by many types of tumor [35]. Therefore, TF may be involved in tumor-related abnormal blood coagulation.

Above all, any malignant tumor can erode the surrounding normal tissue, and the more erosive types of cancer have more destructive actions. If these cancer clusters erode adjacent normal or tumor vessels, microscopic hemorrhage may occur at any

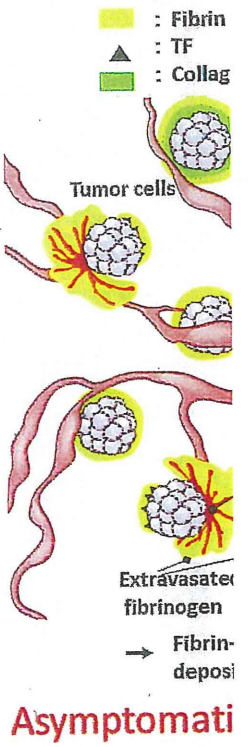

Fig. 6.3 A diagram of the

place and at any time
ately form in situ to st
collagenous stroma in
nonmalignant diseases
diac infarction, brain i
only at the onset or a
digestion or replacem
some symptoms. On t
long as the cancer cel
this "malignant cycle
metastasis progress v
needed). When any sy
tion, or macroscopic b
and destruction of the
of a particular place
cancer receive chemot
patients if they suffer
injury, or active infla

agulation

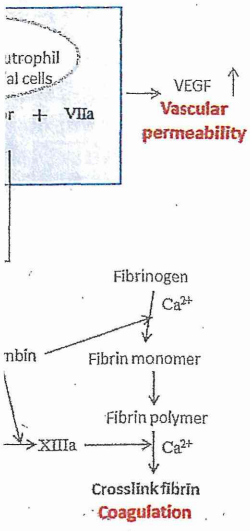

and extrinsic coagulation

rtant event for the EPR
ceeded in purifying two
rom the ascitic fluid of
t this kinin generation
trinsic coagulation fac-

ibility factor (VPF) was
s found that VPF was
. Recently, an extrinsic
activate VEGF produc-
ors may be involved in
coagulation (Fig. 6.2).
sseau described throm-
ne [36]. Today, a large
mal coagulation occurs
is highly expressed on
ly spliced soluble TF is
TF may be involved in

g normal tissue, and the
If these cancer clusters
rhage may occur at any

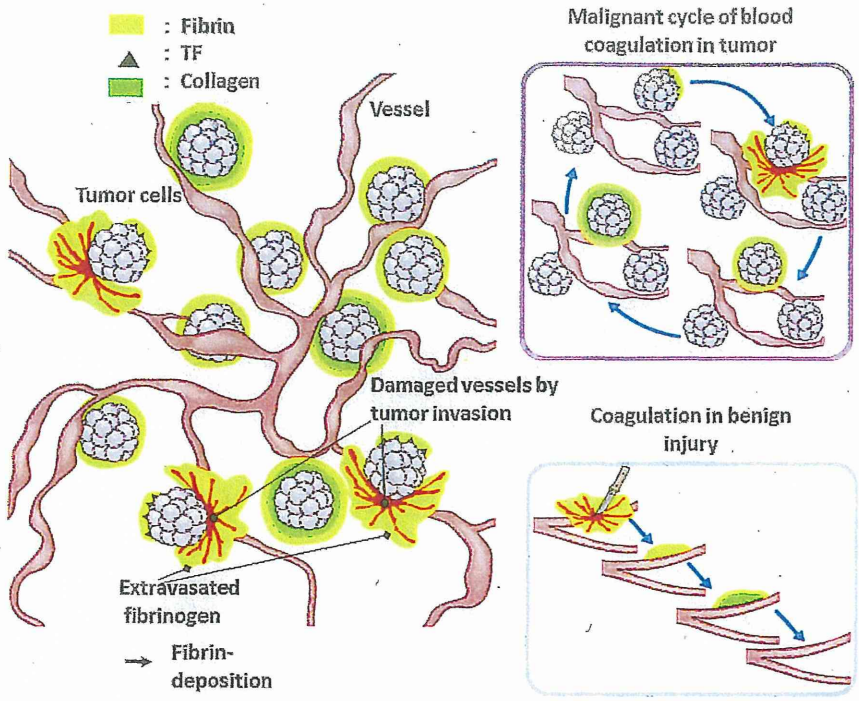

Fig. 6.3 A diagram of the 'malignant cycle of blood coagulation' in cancer tissue

place and at any time within or adjacent to cancer tissues, and fibrin clots immediately form in situ to stop the bleeding. The fibrin clots are subsequently replaced by collagenous stroma in a process similar to that in normal wound healing and other nonmalignant diseases. Fibrin clot formation in nonmalignant disorders such as cardiac infarction, brain infarction, injuries, and active rheumatoid arthritis should form only at the onset or active state of disease and subsequently disappear by plasmin digestion or replacement with collagen within a few weeks and is accompanied by some symptoms. On the other hand, the fibrin clot formation in cancer lasts for as long as the cancer cells survive in the body and occurs silently. Therefore, we call this "malignant cycle of blood coagulation" (Fig. 6.3). In fact, tumor invasion and metastasis progress without symptoms (which is why imaging instruments are needed). When any symptoms accompanying cancer such as pain, intestinal obstruction, or macroscopic bleeding occur, the cancer is likely to involve the sensory nerves and destruction of the bones and larger blood vessels and to occupy the whole lumen of a particular place of the intestine. Usually, patients with an advanced stage of cancer receive chemotherapy and it is worth noting that oncologists never treat such patients if they suffer from existing acute thrombotic complications, bleeding by injury, or active inflammation. Therefore, we conclude that cancer-induced blood

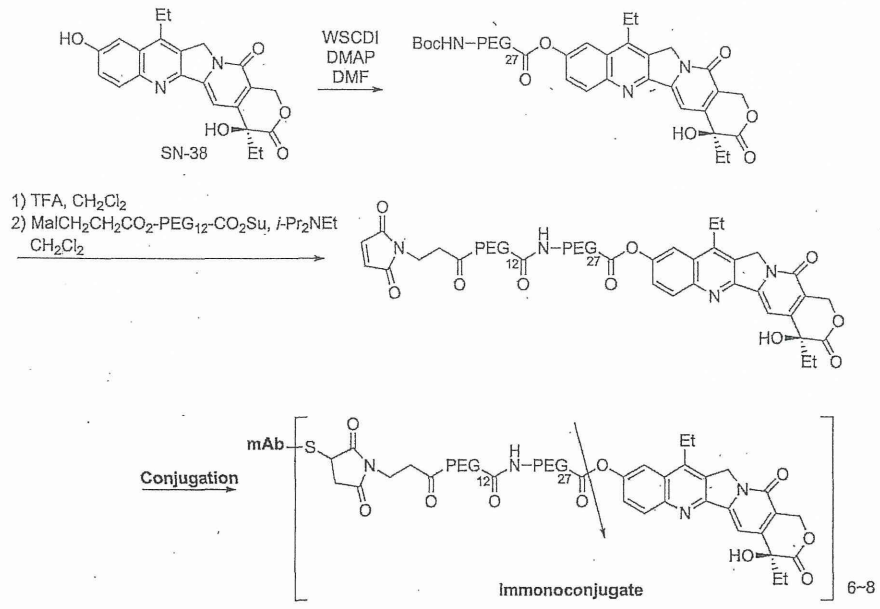

Fig. 6.4 Synthetic scheme of the immunoconjugate. The arrow indicates the cleavage site for releasing free active SN-38. PEG, Polyethylene glycol

coagulation may be an origin of tumor stroma and that fibrin clots in cancer tissues of patients who can receive chemotherapy are actually tumor specific.

CAST Therapy

CAST Therapy Using Anti-collagen 4 mAb

SN-38 is a topoisomerase 1 inhibitor and an active component of CPT-11 which is used clinically for colorectal, lung, and other cancers. For the mAb conjugation to phenol-OH in SN-38, an ester bond was selected. In our design, polyethylene glycol (PEG) was combined close to the bond (Fig. 6.4). PEG is known to evade nonspecific capture by RES. The drug (SN-38)/mAb ratio (the number of drugs attached to a mAb) of each immunoconjugate ranged from 6.7 to 8.4.

Antitumor activities of immunoconjugates with ester bond SN-38 were evaluated in mice bearing human pancreatic tumor genografts. CPT-11 and three immunoconjugates showed significant antitumor activities compared to results in mice treated with saline, in mice bearing either PSN1 (EpCAM positive and stroma poor) or SUIT2 (EpCAM positive and stroma rich) tumors. In SUIT2 tumors, while the tumor continued to increase in mice treated with CPT-11, anti-CD20 immunoconjugate (as a nonspecific control), and anti-EpCAM immunoconjugate, the tumor in

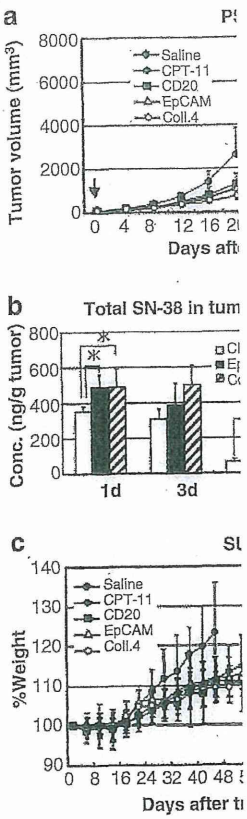

Fig. 6.5 Anti-tumor effect
lagen 4 immunoconjugates
PSN1 and SUIT2, the 3 i
groups of mice by intraver
the curves illustrate the e
EpCAM in PSN1), P<0.01
in SUIT2), P<0.001 (Salin
or EpCAM vs. Collagen 4
and unbound) SN-38 (up
(lower) were determined u
*P<0.05, Bar=SD. (c) Ch
Collagen 4 in the same tre
change of jejunum from n
(lower). Scale bar: 1mm. (

mice treated with anti
month and never resun
(stroma poor), differer
38 immunoconjugate
anti-CD20 or anti-Ep